Northumbria Research Link

Wrinkle-Enabled Highly Stretchable Strain Sensors for Wide-Range Health Monitoring with Big Data Cloud Platform

Jian Huang,[a] Jian Zhou,[*a] Yangmei Luo,[a] Gan Yan,[a] Yi Liu,[b] Yiping Shen,[b] Yong Xu,[c] Honglang Li,[d] Lingbo Yan,[a] Guanhua Zhang,[a] Yongqing Fu,[e] and Huigao Duan[a]

a. State Key Laboratory of Advanced Design and Manufacturing for Vehicle Body, College of Mechanical and Vehicle Engineering, Hunan University, Changsha 410082, China

b. Hunan Provincial Key Laboratory of Health Maintenance for Mechanical Equipment, Hunan University of Science and Technology, Xiangtan 411201, China

c. The Affiliated ZhuZhou Hospital of XiangYa School of Medicine, Central South University, Zhuzhou 412007, China

d. CAS Center for Excellence in Nanoscience, National Center for Nanoscience and Technology, Beijing 100190, China

e. Faculty of Engineering and Environment, Northumbria University, Newcastle upon Tyne, NE1 8ST, United Kingdom

KEYWORDS: strain sensor, wearable electronic, conductive composite, body motion monitoring, wearable Internet of Things

ABSTRACT: Flexible and stretchable strain sensors are vital for emerging fields of wearable and personal electronics, but it is a huge challenge for them to possess both wide-range measurement capability and good sensitivity. In this study, a highly stretchable strain sensor with a wide strain range and a good sensitivity is fabricated based on smart composites of carbon black (CB)/wrinkled Ecoflex. The sensor exhibits a maximum recoverable strain up to 500% and a high gauge factor of 67.7. It has a low hysteresis, a fast signal response (as short as 120 ms) and a high reproducibility (up to 5000 cycles with a strain of 150%). The sensor is capable of detecting and capturing wide-range human activities, from speech recognition, pulse monitoring, to vigorous motions. It is also applicable for real-time monitoring of robot movements and vehicle security crash in an anthropomorphic field. More importantly, the sensor is successfully used to send signals of a volunteer's breathing data to a local hospital in real time through a big-data cloud platform. This research provides the feasibility using strain sensor for wearable internet of things and demonstrates its exciting prospect for healthcare applications.

1. INTRODUCTION

The rising cost of healthcare, the sharp increase in elderly population, and the prevalence of chronic diseases around the world urgently demand the transformation of healthcare from a hospital-centered system to a point-of-care environment, with the help of rapid advances in wearable internet of things (WIoTs).[1,2] The components of WIoTs generally include wearable sensors, internet-connected gateways and the supporting big data cloud platform. The WIoTs will not only continuously monitor the user's health conditions in real time with a function of long-distance data transmission, but also provide timely information of various health parameters to the users and their doctors or physicians.[3,4] Flexible strain sensors are regarded as one of the key WIoTs, which can be designed to attach to a targeted flexible object for the purpose of measuring its deformation in a precise manner. They have wide-range applications for monitoring surface strains of human skin due to joint motion, tissue swelling, wound healing, or even emotional expression.[5-7] Different types of flexible strain sensors have been reported.[8-11] However, practical implementation of these strain sensors for skin-mountable and wearable applications still remains a great challenge due to the sophisticated measurement equipment, poor resolution, and/or poor dynamic performance of the senosrs.[12,13] Currently, resistive strain sensors are regarded as promising and valuable tools for wearable applications, as they require relatively simple read-out systems and structure design, offer the potentially high flexibility, stretchability and high sensitivity, and have simple microfabrication processes.

Recent studies in this field have been focused on using electrically conductive materials coupled with flexible polymers. Various materials such as low-dimensional carbon materials (e.g., carbon black (CB), carbon nanotubes (CNTs) and graphene), nanowires (NWs), nanoparticles (NPs) and their hybrid micro/nanostructures have extensively been investigated to integrate into polymers for fabricating the strain sensors.[10,14-23] For example, Gong, S. et al. reported a AuNWs−latex rubber strain sensor with a gauge factor (GF) of 6.9-9.9 and a stretchability up to 350%.[10] Amjadi, M. et al. fabricated a CNT percolation networks–silicone rubbers train sensor, with a high stretchability up to 500% and a GF of 1-2.5.[7]

For the WIoTs applications, the flexible strain sensors need to have a high sensitivity, large stretchability, and a good stability for long-term repeated usages. Many researchers proposed various methods to significantly improve the sensitivity while achieving a reasonable strain rage and a good durability.[24-28] For example, Liu Q. et al. reported a graphene-based device with a fish-scale microstructure configuration,

and achieved a sensing range up to 82% strain, a GF value of 16.2−150 and excellent reliability and stability (>5000 cycles).[24] Lin, L. et al. proposed a facile preparation method for superhydrophobic and multi-functional conductive nanofiber composites (CNCs) with a dual conductive network, and the CNCs based strain sensor possesses an extremely large GF value of 1.04×10^5, with the strain range from 20% to 70%.[25] Li, Q. et al. developed strain sensors using ultra-violet/ozone (UV/O_3) treated CNT/Ecoflex, and achieved a high sensitivity up to 1020.2 and a stretchability up to 100%.[26] They also used acid-interface engineering method to increase the sensitivity by generating a layer of SiOx at the interface between the CNT film and Ecoflex, and achieved a GF value up to 1665.9, without sacrificing the stretchability (>100%).[27] Nevertheless, most of these sensors still have difficulties to simultaneously achieve high stretchability, full-range of strain detection, high sensitivity, and ultra-fast response time.

In this research, smart composites of CB/wrinkled Ecoflex was proposed and applied as a high-performance strain sensor. CB has merits of low cost, excellent electrical and mechanical properties, high conductivity, good biocompatibility, high mechanical strength and abrasion resistance when it is used as a filler in an elastomeric matrix.[28-30] In addition, a simple and low-cost surface treatment method is proposed to form micro-scale wrinkles and protrusions on the Ecoflex substrate. These can significantly increase specific surface areas and interface bonding between Ecoflex and CB and improve its adhesion onto Ecoflex, without apparently affecting the mechanical properties of Ecoflex substrate. The formed highly stretchable, wide-detection-range and highly sensitive CB-Ecoflex composite strain sensors can be mass produced at a low cost. The CB-Ecoflex based strain sensor exhibited a large stretchability with a maximum recoverable strain up to 500%, a high sensitivity of 67.7 at the strain range of 300%-500%, a fast signal response (e.g., 120 ms) and a high reproducibility (up to 5000 cycles with 150% strain). The applicability of this highly stretchable and sensitive strain sensor was demonstrated by a series of regular human motion detection, vigorous motion detection, real-time monitoring of robot movements and vehicle security crash in an anthropomorphic field. More importantly, we demonstrated its application by combining the CB-Ecoflex composite strain sensor with a big data cloud platform, proving its feasibility for the applications in the Internet of Things (IoT) and telemedicine.

2. EXPERIMENTAL SECTION

2.1. Characterization and Measurements. Top-view and cross-section morphologies of Ecoflex and CB-Ecoflex composites were observed using a scanning electron microscope (SEM, TESCAN Company). Tensile measurement of sensor was carried out using a tensile tester (Shimadzu, model AGS-X, 100 N, China) at room temperature, with a constant velocity of 100 mm min^{-1} and a clamp distance of 2 cm. Electrical signal (resistance change) of strain sensors was recorded using a Keithley 2611B source meter. The adhesion between CB and Ecoflex of the CB-Ecoflex composite was assessed using a coating adhesion test method with a tensile testing machine (ZQ-990A, Dongguan Zhiqu Precision Instruments Co., Ltd.).

2.2. Human Motion Detection Experiment. To demonstrate the potential applications of CB-Ecoflex composite as wearable sensors for wide-range detections of human activities, we assembled the CB-Ecoflex composite strain sensor with elastomeric tape, copper conductive adhesive and wires, and the wires at both ends of the sensor were connected to the Keithley 2611B source meter for sensor data recording. The wearable sensors were conformally attached to different body positions (such as knuckle, back wrist, elbow and knee) of a person using medical tapes. The restriction to skin/body motion was minimal because the device is ultra-light in weight, highly flexible and with a wide-range measurement capability.

2.3. Robot Motion Monitoring and Crash Anthropomorphic Experiment. The composite strain sensor was further implemented for real-time monitoring of complicated and combined movements in robotics. For these studies, the sensor was fixed on the thumb of a manipulator (with the angle of the steering gear from 0°-45°-90°-150°-0°) to control the movement of the object. To demonstrate the ability of the composite strain sensor to monitor external shocks to a car crash test dummy in the field of vehicle security crash anthropomorphic applications, we attached the sensor to chest of the dummy with elastomeric tape, and the dummy was hit with bullets fired from a toy air gun. Each collision of the bullet from the toy air gun simulated the event of vehicle crash.

2.4. Experiment of WIoT application. To demonstrate the WIoT functionality, we sent the signals from the composite strain sensor to a data cloud platform to monitor human breathing status in real time over a long distance. Here we mounted the strain sensor on the abdomen of a volunteer in Hunan University (Changsha, China) to monitor breathing. Data obtained from the sensors were collected and analyzed using Huygens Bridge circuit, amplifier circuit, A/D conversion, signal processing chip. The data were then sent to the Data Transfer unit (DUT) and further transmitted to the Big Data Cloud Platform in the ZhongDa Testing Technology Group (about 10 km away from Hunan university). The cloud platform remotely monitored human breathing status in real time from a long distance. When the data showed abnormal values, an urgent alert was triggered, which was monitored by a doctor in the Affiliated ZhuZhou Hospital, Zhuzhou, 58 km away from the company and 62 km away from the Hunan University. The doctor then sent the treatment information back to the volunteer who was in Hunan university. The doctor continuously monitored the sensing data through the big data cloud platform and provided the real time treatment for the volunteer which was 62 km away.

3. RESULTS AND DISCUSSION

3.1. Fabrication of Wrinkle-Enabled Highly Stretchable Strain Sensor. Figure 1a schematically illustrates fabrication procedures of wrinkle-enabled CB-modified Ecoflex composite, and the detailed fabrication procedures can be obtained from the Supporting Information (SI). In the first step, Ecoflex liquid (00-30) was transferred onto the grooves of a 3D printed mold and cured at room temperature for 3 hrs to form a solid Ecoflex elastomer. The obtained solid Ecoflex was then immersed in a toluene solution for 3.5 hours, and the dimension of Ecoflex was increased by 1.5-1.6 times, forming a swollen Ecoflex elastomer as shown in **Figure 1**b. To compare the strain sensitivity for the Ecoflex with wrinkles and without wrinkles, two types of Ecoflex (CB-Ecoflex A and CB-Ecoflex B) were developed. Compared with the Ecoflex A, the Ecoflex B was modified with toluene to form surface wrinkles and protrusions, thus it adsorbed more CB particles in the later process stage and the color was much darker as shown in **Figure 1**b.

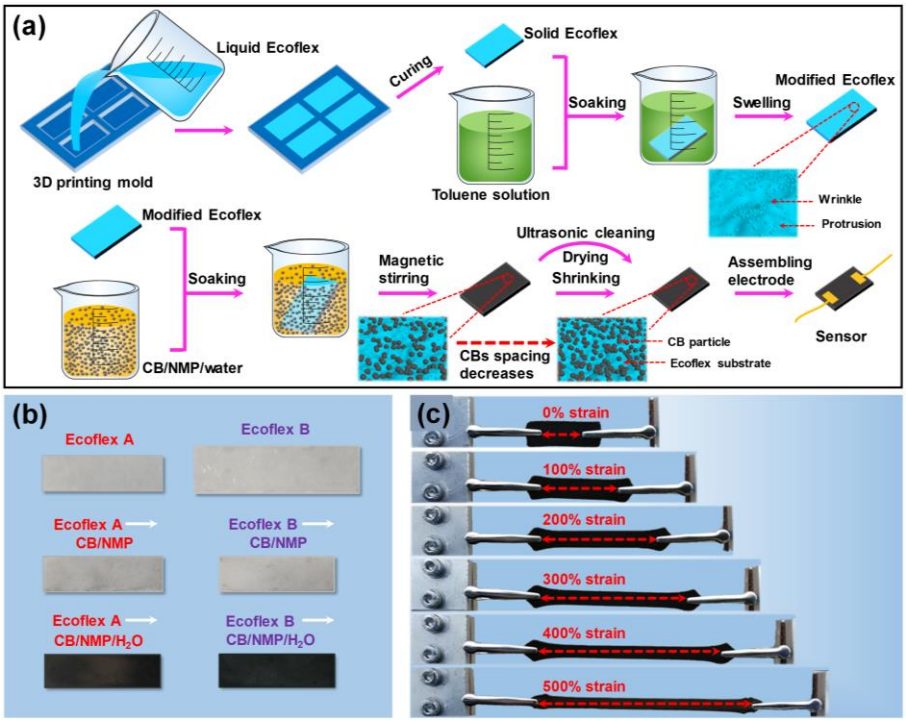

Figure 1. Fabrication processes and result of CB-Ecoflex composite. (a) Schematics of the fabrication of conductive CB-Ecoflex composite. (b) Photographs of conductive CB-Ecoflex composite at different fabrication stages (Left to right: Ecoflex A, Ecoflex A after being stirred in CB: NMP solution, Ecoflex A after being stirred in CB: NMP: water solution, Ecoflex B (being immersed in a toluene solution for 3 hours), Ecoflex B after being stirred in CB: NMP solution and Ecoflex B after being stirred in CB: NMP: water solution). (c) Photographs of the CB-Ecoflex composite strain sensor after being stretched to different strains: ε= 0%, 100%, 200%, 300%, 400% and 500%, respectively.

CB was added into a mixed solution of N-methyl-pyrrolidone (NMP) and deionized water to form the CB: NMP: water dispersion solution. The role of NMP is to dissolve the CB particles to form a CB solution, and that of water is to reduce the solubility of CB in NMP and effectively transfer the CB particles from NMP to Ecoflex (see SI). Without water, the Ecoflex cannot effectively adsorb much carbon black after stirred in CB: NMP solution, which shows that water is energetically favorable for the CB to be attached to the Ecoflex as shown in **Figure 1**b.

For fabrication of strain sensors, the prepared Ecoflex was immersed into the CB:NMP:water solution, and was further stirred at room temperature for 3 hrs using a magnetic stirrer. This will promote the CB's adsorption onto the surface of Ecoflex elastomer. The prepared sample was ultrasonically cleaned with deionized water and dried in a vacuum oven to obtain the CB-Ecoflex composite. **Figure 1**c shows photos of the CB-Ecoflex composite strain sensor with stretched strains of ε= 0%, 100%, 200%, 300%, 400% and 500%, respectively, which clearly shows the good stretchability properties of CB-Ecoflex composite strain sensor.

3.2. Effects of Surface Modification of Ecoflex on Piezoresistivity of CB-Ecoflex Sensor. Figure 2a shows resistance values of different types of CB-Ecoflex composites prepared in CB: NMP: water solution with NMP/water ratios of 1:1 (A1, B1) and 1:4 (A2, B2) and a CB concentration of 2 mg/ml (Here, A and B represent CB-Ecoflex A and CB-Ecoflex B, respectively, which are described in detail in the Experimental Section). It is clear that the resistance of CB-Ecoflex B (modified with toluene) is much smaller than that of CB-Ecoflex A. This is because when the Ecoflex was soaked with toluene, the dimension of Ecoflex was increased by 1.5-1.6 times and then protrusions and wrinkles were formed on the surface of the Ecoflex. This resulted in significant increases in the surface area of Ecoflex and also the interfacial bonding between Ecoflex and CB, thus leading to more CB absorbed onto the surface of the Ecoflex. These changes significantly decrease the resistance and increase the conductivity. The results show the same trend for two samples treated with different NMP/water ratios (1:1 and 1:4). **Figure 2**b shows relative resistance changes ($\Delta R/R_0$) of two types of CB-Ecoflex composites which were stirred in NMP/water=1/1 and NMP/water=1/4. The GF of the strain sensor was calculated, which is defined as $(\Delta R/R_0)/\varepsilon$, where $\Delta R/R_0$ is the relative resistance change, and ε is strain. The GF values of CB-Ecoflex A1, B1, A2, B2 are 3.9, 4.1, 4.1, 10.8 (strain range: 0%-100%) and 3.9, 7.2, 4.1, 21.4 (strain range: 100%-240%), respectively, indicating that NMP/water ratio of CB dispersion solution has a significant influence on the performance of the sensor. The CB-Ecoflex B has larger values of GF because the Ecoflex has been soaked with toluene to form the protrusions and wrinkles and thus the interface bonding between Ecoflex and CB has been significantly improved. The larger GF values indicate that the sensor could have a better sensitivity. Furthermore, we have obtained the largest GF of 67.7 with the NMP/water value of 1/4, in the strain range of 300%-500%.

Figures 2c and **2**d show the SEM images of cross-section microstructures of the Ecoflex before and after soaked with toluene. The surface of original Ecoflex is smooth. Whereas that of Ecoflex after toluene treatment shows many protrusions and wrinkles, which significantly increase the specific surface areas and provide an excellent condition for Ecoflex to adsorb more CB particles onto its surface. The wrinkled structure was formed by the pre-stretching and shrinkage of Ecoflex,

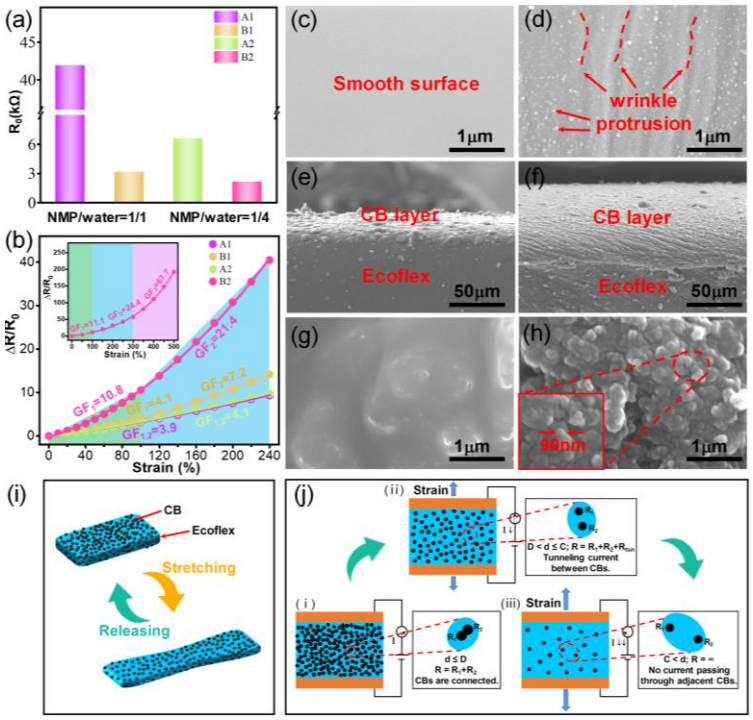

Figure 2. (a) The initial resistance and (b) the $\Delta R/R_0$ curves of two types of CB-Ecoflex composites treated in different NMP/water ratios (NMP/water=1/1, 1/4) of CB solution. The inset figure is $\Delta R/R_0$ curve of CB-Ecoflex composites (NMP/water=1/4, B2) with the strain up to 500%. (c) SEM images of the surface of Ecoflex (without soaked in toluene); (d) the surface of Ecoflex (with soaked in toluene); (e) the cross-section morphology of CB-Ecoflex (without soaked in toluene) composite; (f) the cross-section morphology of CB-Ecoflex (with soaked in toluene) composite; (g) the surface of CB-Ecoflex (without soaked in toluene) composite and (h) the surface of CB-Ecoflex (with soaked in toluene) composite. (i) Schematic illustration of sensing mechanism of conductive CB-Ecoflex composite strain sensor under stretching-releasing process. (j) Different electrical interconnections between two adjacent CB: (i) a full contact; (ii) a tunneling junction within a certain cut-off distance C; and (iii) a complete disconnection between CB NPs.

whereas the protrusions was produced because of the removal of toluene which was pre-diffused inside Ecoflex during soaking stage. **Figures 2**e and **2**f show that with the same soaking time of CB: NMP dispersion solution, the Ecoflex treated with toluene has absorbed more CB particles and the CB particles layer is much thicker. The increased thickness of CB particles will lead to a lower resistances of CB-Ecoflex composites, as only the CB particles are conductive in the CB-Ecoflex composite. **Figures 2**g and **2**h present surface morphologies of the CB-Ecoflex composite before and after toluene treatment. The CB particles are easily agglomerated in the form of a cluster on the surface of untreated Ecoflex, whereas the CB particles are well-dispersed as nanoparticles (with the size of 90 nm) on the toluene treated Ecoflex. The protrusions and wrinkles formed on the surface of Ecoflex increase the specific surface area for the adsorption of CB, and increase the stability of the adsorption of Ecoflex and CB, which effectively inhibit the agglomeration of CB particles. When the CB particles are formed as a cluster on the Ecoflex, it will inhibit further adsorption of CB particles and result in a decreased conductivity. Also, with these cluster formed on the surface, the average distance between CB particles will show little changes when the composite is stretched. This will result in a smaller change in conductive percolation pathways, thus causing a relatively lower strain sensitivity. Therefore, the agglomerated CB clusters are not good for the performance of strain sensors. The CB particles in the state of separated nanoparticles on the Ecoflex composite surface has shown better conductivity and sensitivity.

To verify the effect of toluene treatment on interfacial bonding between CB and Ecoflex, we have used the coating adhesion testing method to characterize the adhesion between CB and Ecoflex of the CB-Ecoflex composite. The obtained results are shown in **Figure S1**. The average value of interfacial bonding force of CB-Ecoflex B (soaked in toluene to form the protrusions and wrinkles) is ~ 4.7 N, which is nearly five times as large as that of CB-Ecoflex A (~0.95 N, without protrusions and wrinkles). This clearly demonstrates that by soaking the Ecoflex in toluene to form wrinkled structures, the bonding and adhesion between Ecoflex and CB can be significantly improved.

Figures 2i and **2**j illustrate the sensing mechanism of the conductive CB-Ecoflex composite strain sensor under stretching-releasing processes. The mechanism of CB-Ecoflex strain sensor is based on the formation of a conductive network and deformation-induced changes in the tunneling conductance of the closely spaced nanoparticles.[31, 32] As shown in **Figure 2**i, before stretching, the Ecoflex elastomer surface is covered by many closely packed CB nanoparticles. These will form a good conductive network, which results in a low value of electrical resistance. However, this network is gradually elongated and finally broken when the strain sensor is gradually stretched. This will enlarge the spacing of the CB nanoparticles, thus leading to the increase of the resistance of the strain sensor. As shown in **Figure 2**j, the junctions between two adjacent CB particles can be classified into three categories depending on their distances, e.g., (i) a full contact; (ii) a tunneling junction within a certain cut-off distance C; and (iii) a complete disconnection between CB

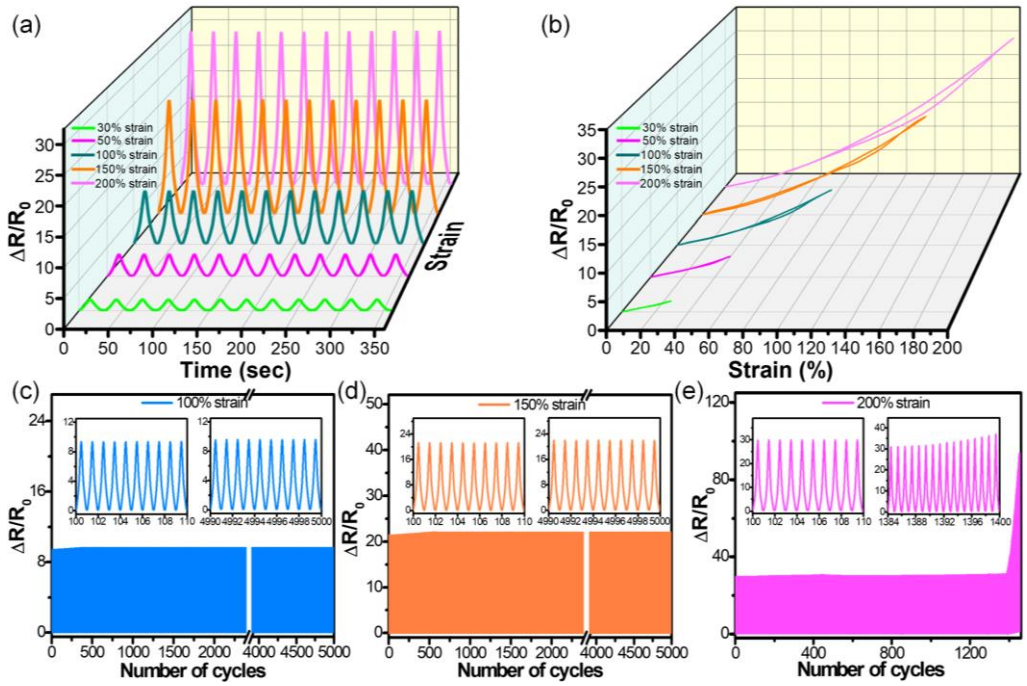

Figure 3. Electromechanical characterization of the CB–Ecoflex composite based strain sensor. (a) The ΔR/R0 curve of the CB-Ecoflex composite strain sensor during 12 cycles of loading−unloading under different strains (30, 50, 100, 150 and 200%). (b) Hysteresis curve for the CB-Ecoflex composite strain sensor under different strains. (c) The cycling durability curve of the strain sensor under 100% strain, (d) 150% strain and (e) 200% strain (stretching rate of 100 mm min^{-1}).

NPs. Firstly, If the shortest distance d between the centerlines of two neighboring CB particles is smaller than or equal to the diameter (D) of CB NP, these NPs are considered to be fully connected with a low contact resistance. Secondly, when the distance d is larger than D but smaller than a cut-off distance C, the tunneling of currents between these two noncontact CB particles can be triggered, and electrons can be tunneled through the polymer matrix, thus forming a quantum conductive junction. Finally, when the distance among CBs exceeds the cut-off distance C, it is assumed that no current can pass through two adjacent CBs and their electrical path is fully disconnected.[6]

The mechanism of conductive CB-Ecoflex composite strain sensor should be explained as follows. Before stretching, the Ecoflex elastomer surface is covered by many closely packed CB nanoparticles, thus forming a perfect conductive network. In such a condition, a full contact between two adjacent CB particles will result in a low value of initial resistance. When the CB-Ecoflex composite is stretched with a relatively small strain, some previously closely packed CB nanoparticles are gradually separated and gaps of several nanometers are formed, thus causing tunneling currents.[33,34] Within these small strain ranges, the junctions between adjacent CB particles are either in a full contact mode or tunneling junction, so the resistance of the composite will increase slightly as a function of strain. With further increase in tensile strain, more CB nanoparticles are gradually separated, and the junctions between adjacent CB particles are changed from a full contact mode to tunneling junctions. In this strain range, the major types of junctions are tunneling junctions, thus the resistance is significantly increased. With the further increase of the strain, the distances between many adjacent CB particles start to be larger than the cut-off distance, e.g., their electrical paths are disconnected. In this large strain range, the major types of junctions are either tunneling junctions or completely disconnected, thus leading to very large resistance. After the CB-Ecoflex composite is released from the stretched conditions and returns to its original state, the distances between adjacent CB particles return to their initial values, and hence the resistance values have been recovered. In brief, with the increase of strain, the dominant junctions between two adjacent CB particles will be gradually changed from a full contact mode, to the tunneling junction, and finally to a complete disconnection mode. Accordingly, the resistance changes show different linear regions at different strain ranges.

3.3. Electromechanical Performance of CB-Ecoflex Composite Strain Sensor. Figure S2 in the **SI** shows the results for optimization of parameters of CB concentration and NMP/water ratio, which can achieve the best performance of the composite strain sensor. As the optimal CB concentration was found to be 2 mg/ml and the optimal NMP/water ratio of CB dispersion solution to be 1/4, we chose these parameters to fabricate the CB-Ecoflex composite and the strain sensor.

Figure 3a shows the relative resistance changes of a CB-Ecoflex strain sensor under cyclic stretching–releasing at different strains with the same frequency. The resistance changes are increased as the strain is increased, but the value can be fully recovered after each of cyclic stretching–releasing process. **Figure 3**b illustrates the hysteresis curves of the composite strain sensor. The hysteresis is quite small (less than 4% for strain sensor) when the strain range is less than 150% in response to the stretch/release cycles. For a larger strain such as ε= 200%, although the hysteresis error is relatively large, the resistance value can still be fully recovered after stretch/release cycles, showing the outstanding stretchability of the strain sensor.

A strain sensor needs to maintain its sensing characteristics without apparent fatigue failure for real-life applications. To investigate the long-term stability of the strain sensor, 5000

cycles of repeated stretching/releasing processes with a maximum strain of ε= 150% was applied to the sensor at a

Table 1. Comparisons of device performance of different resistance-type stretchable strain sensors.

Materials	Gauge factor	Stretchability	Response time (ms)	Cyclic stability	Ref.
PDMS/AgNWs/PDMS	2 ~ 14	70%	200	1000 cycles (10%-40%)	[6]
CNTs/Ecoflex	1 ~ 2.5	500%	Unmentioned	2000 cycles (0%-300%)	[7]
SiO_2 NPs/graphene shell/PU nanofiber	5.9	110%	Unmentioned	600 cycles (0%-50%)	[17]
SiC/Ecoflex	2.47×10^5	5%	200	10000 cycles (0-4%)	[19]
Fragmented SWCNT paper/PDMS	10^7 (0%-50% strain)	50%	300	10000 cycles (0-20%)	[23]
ACNTs/AgNPs/PDMS/ TPU nanofiber	1.04×10^5 (20%-70% strain)	476%	Unmentioned	1000 cycles (0%-70%)	[25]
ultra-violet/ozone cracked CNTs/Ecoflex	1020.2	100%	Unmentioned	10000 cycles (25%-70%)	[26]
Acid-Interface Engineering of CNT/Ecoflex	35.2 (0%-80% strain) 129.1 (80%-120% strain) 1665.9 (>120% strain)	>100%	Unmentioned	10000 cycles (0-80%)	[27]
RB/CBNPs/PDMS	242.6 (38.8%–71.4% strain)	980%	Unmentioned	1000 cycles (0%-50%)	[28]
CBs/Ecoflex	3.8	400%	Unmentioned	1000 cycles (0%-1%)	[29]
CB/wrinkled Ecoflex	67.7 (300%-500% strain)	500%	120	5000 cycles (0%-150%) 1390 cycles (0%-200%)	This work

a) RB/CBNPs/PDMS: Rubber band/carbon black nanoparticles/PDMS. PU nanofiber: Polyurethane nanofiber.

b) ACNTs: Acid modified carbon nanotubes. TPU nanofiber: Thermoplastic polyurethanes nanofiber.

stretching–releasing sweeping speed of 100 mm min^{-1}. The obtained results are shown in **Figures 3**c and **3**d. The strain sensor shows a good stability with the maximum change ratio of the normalized resistance ($\Delta R/R_0$) of 0.001 during 5000 cycles of stretching/releasing without apparent failure. From the experimental results, we could verify that our strain sensor has a good mechanical durability against repeated elongation/relaxation cycles, without apparent long-term drifting when the strain is less than 150%. Even under a large strain of 200%, the strain sensor can still maintain a good performance up to 1390 cycles (**Figure 3**e), demonstrating its good mechanical durability and stability.

The response time of CB- Ecoflex strain sensor was also measured and the obtained results are shown in **Figure S3.** Results showed that the response time of the proposed strain sensor can be as short as 120 ms, demonstrating its fast response. We have summarized these results and also compared the performance of resistance-type stretchable strain sensors reported in literature (see **Table 1)**. It is clearly seen that our device has the overall performance of high sensitivity, wide detection range and fast response time.

3.4. Applications for Human Motion Detection, **Intelligent Robotic and Crash Anthropomorphic.** The wearable sensors were conformally attached to different positions of a volunteer's body to monitor motions. For the motion sensing, the wearable sensors were fixed onto the knuckle (**Figure 4**a), wrist (**Figure 4**b), elbow (**Figure 4**c), and knee (**Figure S4a**). **Figure 4**a presents the changes of resistance signals of the strain sensor by applying the sensor on the index finger. When the finger was bent to a certain angle (e.g., 45°), the relative resistance change of the strain sensor was increased to a certain value and then remained stable. Further bending (90°) would lead to an increase in the resistance, forming a stepwise signal. The results of signals show good repeatability and stability of the data obtained from the strain sensor. Similar measurements were conducted on wrist (**Figure 4**b) and elbow (**Figure 4**c**)** with a continuous bending, and the strain sensor also exhibited good performance and repeatable results. In **Figure S4a**, the sensor correctly recorded and identified various knee-related motions such as knee flexing/extending (half squat and full squat), by virtue of the distinctly different patterns of response curves. This demonstrates the ability of the strain sensor to monitor a large deformation of human body.

For monitoring subtle physiological signals from human body, we attached the wearable sensors to the wrist and recorded the wrist pulse under normal/exercise conditions. The obtained current signal results are shown in **Figure S4b**. The amplitude and frequency of pulse were recorded in real time (each peak denotes one pulse). Under the relaxation condition, it was calculated to be 72 beats/min, whereas after exercise, both frequency and amplitude of the signals were significantly increased, with an increased pulse frequency of 96 beats/min.

The sensors can also monitor the breathing and swallowing movements (**Figure 4**d). We attached the sensor near the throat to record the signals. As shown in **Figure 4**e, when the wearer spoke different words, such as "Hello", "Apple" and "Sensor", the response signal curves exhibited characterized patterns with a good repeatability. The signal changes are mainly resulted from the complicated epidermis/muscle movements around throat during the phonation processes. In literature, so far there are limited reports of wearable sensors with capability of specific phonation recognition, and our

studies provide application potentials in aided speech rehabilitation training and human–machine interactions.

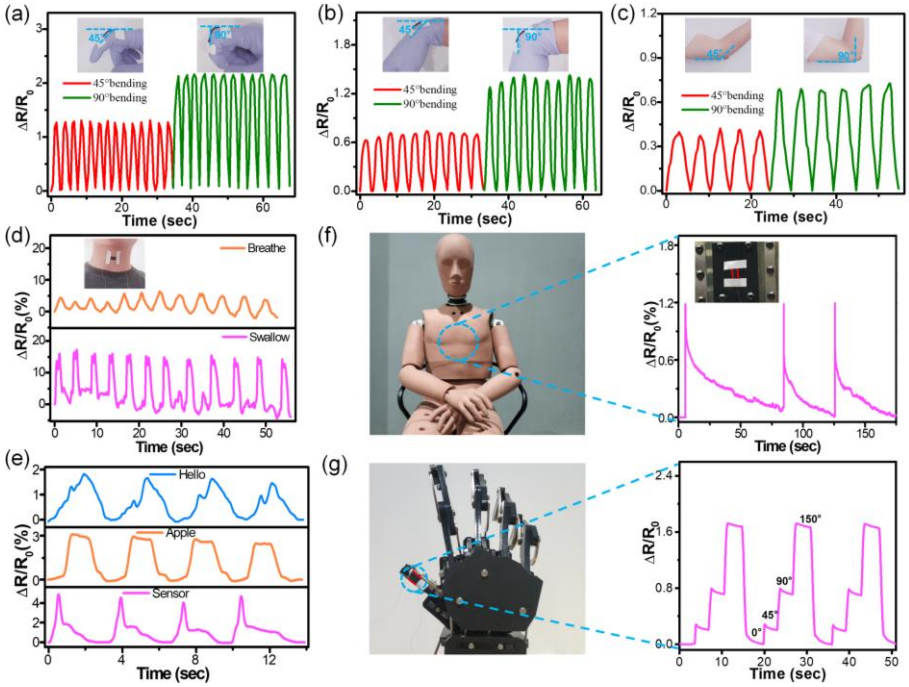

Figure 4. Application of CB-Ecoflex composite strain sensor in monitoring various human motion, intelligent robotic and crash anthropomorphic: real-time relative resistance change of (a) index finger bending, (b) wrist, (c) elbow bending, (d) throat movement (deep breathing and swallowing), (e) phonating, (f) the collision simulation behavior of hitting the robot with an air gun, and (g) the posture simulation behavior of manipulator thumb bending. Insets: digital images of various human motions, robot and manipulator.

We further used our sensor to monitor the anthropomorphic process of car crash. **Figure 4**f exhibits the signal responses of the strain sensor by applying the sensor to the robot, which was hit with bullets fired from a toy air gun. Each collision of bullet from the toy air gun simulated the vehicle crash. The results clearly demonstrated the ability of the CB-Ecoflex composite strain sensor to monitor external shocks to the car dummy and showed the potential application in the field of vehicle security crash anthropomorphic.

In addition to wearable sensing for humans and vehicle security crash anthropomorphic situation, the CB-Ecoflex composite strain sensor was further implemented for real-time monitoring of complicated movement combination in robotics. The measurement results for the real-time detection of the complete set of movements during the robot finger movement are shown in **Figure 4**g. The results indicate the potential applications of the strain sensor in rehabilitation training for disabled persons and posture simulation.

3.5. Integration with Data Cloud Platform and Wearable IoT. As the composite strain sensor has excellent signal monitoring ability and outstanding stretchability, it is suitable to be integrated with the data cloud platform to form the wearable IoT. Furthermore, this sensor has a simple preparation process and low cost, which is good for mass production in personalized distributed (home) medical treatment, universal basic data monitoring and big data analysis. In this work, we applied the composite strain sensor to data cloud platform to monitor human breathing status in real time over a long distance (shown in **Figure 5**), as the breathing status is symptom of the several serious diseases (e.g., coronavirus pneumonia (COVID-19), or sleep apnea syndrome).

As shown in **Figure 5**a, we mounted the CB-Ecoflex composite strain sensor on the abdomen of volunteers to monitor breathing. **Figures 5**b and **5**c show real-time respiratory data obtained on cloud data platform using the CB-Ecoflex composite strain sensor. When in a normal breathing state, the sensor detected about 16 breaths per minute, while in an obstructed breathing state, sensor detected about 6 breaths per minute. We further sent the signals obtained from the composite strain sensor to the big data cloud platform and achieved real-time/remote monitoring of breathing sensing data over a distance of 62 km (e.g., from the location of volunteer at Hunan University, Changsha, to the doctors of Zhuzhou Central Hospital, ZhuZhou). When the sent data show abnormal values, an urgent alert can be triggered by the doctor, who can then send treatment information back to volunteer. We have realized the basic functions of the WIoTs and verified the feasibility and effectiveness of flexible sensors for the WIoT applications, which has great practical significance and application prospects for realizing real-time monitoring of children's sleep and breathing, for example.

4. CONCLUSION

In summary, we proposed an approach to significantly enhance the sensitivity for full-range measurement and highly sensitivity of CB-Ecoflex strain sensor via introducing protrusions and wrinkles on the surface of the Ecoflex, using a low-cost fabrication process. The composite strain sensor exhibits a recoverable stretchability up to 500% strain and a gauge factor up to 67.7. It also shows a fast signal response (e.g., 120 ms) and a high reproducibility (up to 5000 cycles with 150% strain), with a negligible hysteresis (e.g., 4%) at a large strain level (150%).

The sensors are capable of detecting and capturing full-range human activities, from speech recognition, pulse monitoring, to vigorous motions (such as knuckle, back wrist, elbow and knee bending). We further apply our sensors for real-time monitoring of robot movements and vehicle security crash in an anthropomorphic field. Finally, we successfully

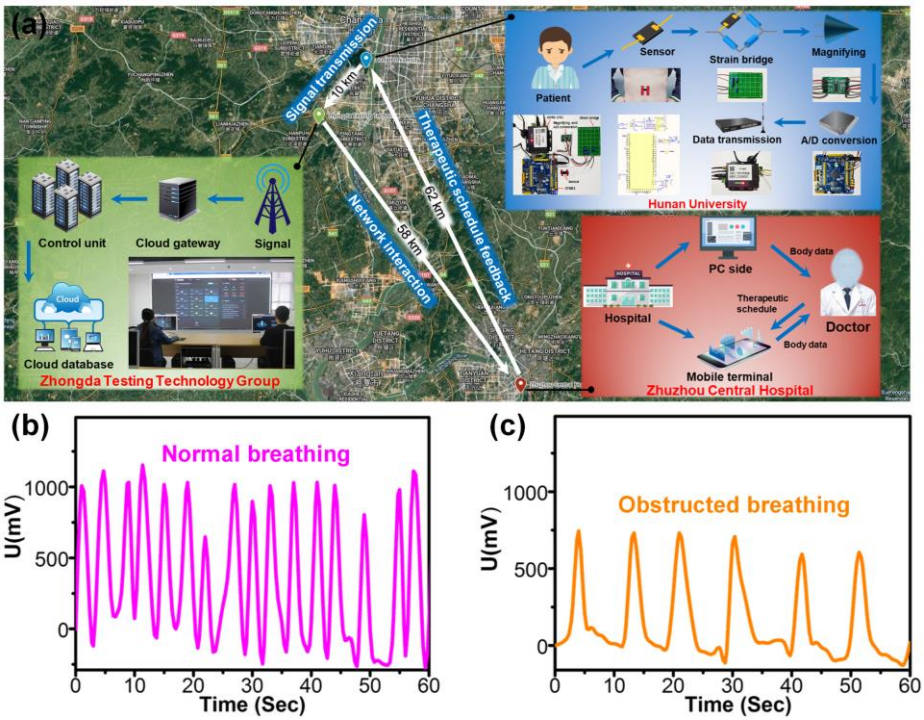

Figure 5. The CB-Ecoflex composite based strain sensor integrates with data cloud platform to monitor human breathing. (a) Schematics of flexible strain resistance sensor for cloud data platform. (b) The real-time normal breathing sensing data and (c) obstructed breathing sensing data on cloud data platform.

integrate CB-Ecoflex composite strain sensor with data cloud platform, demonstrating that the sensor can successfully send signals of a volunteer's breathing data collected to a local hospital in real time through big-data cloud platform, with a long distance of 62 km. It is believed that such a simple and cost-effective fabrication protocol provides new insights into the design of highly elastic conductive polymer nanocomposites for use as flexible and stretchable strain sensors for future wearable electronics. We believe the work has its practical significance and application prospects for the development of wearable flexible sensors for wearable heath Internet of Things.

ASSOCIATED CONTENT

Supporting Information

The detailed fabrication process of CB/wrinkled Ecoflex composite strain sensor; Hansen solubility parameters of the various substances and their effects in this work; Interfacial bonding force between CB and Ecoflex of the CB-Ecoflex composite; Effects of CB concentration, NMP/water ratio of CB/NMP dispersion solution on the performance of CB-Ecoflex composite strain sensor; Response time of CB-Ecoflex composite strain sensor; Other data of CB-Ecoflex composite strain sensor about applications for human motion detection.

AUTHOR INFORMATION

Corresponding Author

*E-mail: jianzhou@hnu.edu.cn.

Author Contributions

The manuscript was written through contributions of all authors. All authors have given approval to the final version of the manuscript.

Notes

The authors declare no competing financial interests.

ACKNOWLEDGMENT

This work was supported by the Key Research Project of Hunan Province (2019GK2111, 2018GK2044), The UK Engineering and Physical Sciences Research Council (EPSRC) grants EP/P018998/1, Newton Mobility Grant (IE161019) through Royal Society and the National Natural Science Foundation of China. The authors acknowledge Zhongda Test Technology Group, Engineering Research Center of Automotive Electrics and Control Technology of Ministry of Education and National Engineering Research Centre for High Efficiency Grinding, Hunan University.

REFERENCES

(1) Trung, T. Q.; Lee, N. Flexible and Stretchable Physical Sensor Integrated Platforms for Wearable Human-Activity Monitoringand Personal Healthcare. *Adv. Mater.* **2016**, 28, 4338-4372.

(2) Amjadi, M.; Kyung, K.; Park, I.; Sitti, M. Stretchable, Skin-Mountable, and Wearable Strain Sensors and Their Potential Applications: A Review. *Adv. Funct. Mater.* **2016**, 26, 1678-1698.

(3) Xu, S.; Jayaraman, A.; Rogers, J. A. Skin Sensors Are the Future of Health Care. *Nature* **2019**, 571, 319-321.

(4) Son, D. H.; Lee, J.; Qiao, S.; Ghaffari, R.; Kim, J.; Lee, J. E.; Song, C.; Kim, S. J.; Lee, D. J.; Jun, S. W. Multifunctional Wearable Devices for Diagnosis and Therapy of Movement Disorders. *Nat. Nanotechnol.* **2014**, 9, 397-404.

(5) Lu, Y.; Qu, X.; Zhao, W.; Ren, Y.; Si, W.; Wang, W.; Wang, Q.; Huang, W.; Dong, X. Highly Stretchable, Elastic, and Sensitive

MXene-Based Hydrogel for Flexible Strain and Pressure Sensors. *Research* **2020**, 2020, 2038560.

(6) Amjadi, M.; Pichitpajongkit, A.; Lee, S.; Ryu, S.; Park, I. Highly Stretchable and Sensitive Strain Sensor Based on Silver Nanowire-Elastomer Nanocomposite. *ACS Nano* **2014**, 8, 5154-5163.

(7) Amjadi, M.; Yoon, Y. J.; Park, I. Ultra-Stretchable and Skin-Mountable Strain Sensors Using Carbon Nanotubes-Ecoflex Nanocomposites. *Nanotechnol.* **2015**, 26, 375501.

(8) Kim, M.; Alrowais, H.; Brand, O. 3D-Integrated and Multifunctional All-Soft Physical Microsystems Based on Liquid Metal for Electronic Skin Applications. *Adv. Electron. Mater.* **2018**, 4, 1700434.

(9) Xu, H.; Dong, S.; Xuan, W.; Farooq, U.; Huang, S.; Li, M.; Wu, T.; Jin, H.; Wang, X.; Luo, J. J. Flexible Surface Acoustic Wave Strain Sensor Based on Single Crystalline LiNbO3 Thin Film. *Appl. Phys. Lett.* **2018**, 112, 093502.

(10) Gong, S.; Lai, D. T. H.; Su, B.; Si, K. J.; Ma, Z.; Yap, L. W.; Guo, P.; Cheng, W. Highly Stretchy Black Gold E-Skin Nanopatches as Highly Sensitive Wearable Biomedical Sensors. *Adv. Electron. Mater.* **2015**, 1, 1400063.

(11) Raju, A. P.; Lewis, A.; Derby, B.; Young, R. J.; Kinloch, I. A.; Zan, R.; Novoselov, K. S. Wide-Area Strain Sensors Based Upon Graphene-Polymer Composite Coatings Probed by Raman Spectroscopy. *Adv. Funct. Mater.* **2014**, 24, 2865-2874.

(12) Rahimi, R.; Ochoa, M.; Yu, W.; Ziaie, B. Highly Stretchable and Sensitive Unidirectional Strain Sensor Via Laser Carbonization. *ACS Appl. Mater. Interfaces.* **2015**, 7, 4463-4470.

(13) Zhong, J.; Zhang, Y.; Zhong, Q.; Hu, Q.; Hu, B.; Wang, Z. L.; Wang, Z. L.; Zhou, J. Fiber-Based Generator for Wearable Electronics and Mobile Medication. *ACS Nano* **2014**, 8, 6273-6280.

(14) He, Z.; Zhou, G.; Byun, J.; Lee, S.; Um, M.; Park, B.; Kim, T.; Lee, S. B.; Chou, T. W. Highly Stretchable Multi-walled Carbon Nanotube/Thermoplastic Polyurethane Composite Fibers for Ultrasensitive, Wearable Strain Sensors. *Nanoscale* **2019**, 11, 5884-5890.

(15) Yang, Y.; Shi, L.;Cao, Z.; Wang, R.; Sun, J. Strain Sensors with a High Sensitivity and a Wide Sensing Range Based on a Ti3C2Tx(MXene) Nanoparticle–Nanosheet Hybrid Network. *Adv. Funct. Mater.* **2019**, 29, 1807882.

(16) Qiu, A.; Li, P.; Yang, Z.; Yao, Y.; Lee, I.; Ma, J. A Path Beyond Metal and Silicon:Polymer/Nanomaterial Composites for Stretchable Strain Sensors. *Adv. Funct. Mater.* **2019**, 29, 1806306.

(17) Gao, J.; Li, B.; Huang, X.; Wang, L.; Lin, L.; Wang, H.; Xue, H. Electrically Conductive and Fluorine Free Superhydrophobic Strain Sensors Based on Sio2/Graphene-Decorated Electrospun Nanofibers for Human Motion Monitoring. *Chem. Eng. J.* **2019,** 373, 298-306.

(18) Kim, K.; Jang, N.; Ha, S.; Cho, J. H.; Kim, J. Highly Sensitive and Stretchable Resistive Strain Sensors Based on Microstructured Metal Nanowire/Elastomer Composite Films. *Small* **2018**, 14, 1704232.

(19) Gao, Y.; Li, Q.; Wu, R.; Sha, J.; Lu, Y.; Xuan, F. Laser Direct Writing of Ultrahigh Sensitive SiC-Based Strain Sensor Arrays on Elastomer toward Electronic Skins. *Adv. Funct. Mater.* **2019**, 29, 1806786.

(20) Zhou, J.; Xu, X.; Xin, Y.; Lubineau, G. Coaxial Thermoplastic Elastomer-Wrapped Carbon Nanotube Fibers for Deformable and Wearable Strain Sensors. *Adv. Funct. Mater.* **2018**, 28, 1705591.

(21) Lee, J.; Kim, S.; Lee, J.; Yang, D.; Park, B. C.; Ryu, S.; Park, I. A Stretchable Strain Sensor Based on a Metal Nanoparticle Thin Film for Human Motion Detection. *Nanoscale* **2014**, 6, 11932-11939.

(22) Yan, C.; Wang, J.; Kang, W.; Cui, M.; Wang, X.; Foo, C. Y.; Chee, K. J.; Lee, P. S. Highly Stretchable Piezoresistive Graphene–Nanocellulose Nanopaper for Strain Sensors. *Adv. Mater.* **2014**, 26, 2022-2027.

(23) Zhou, J.; Yu, H.; Xu, X.; Han, F.; Lubineau, G. Ultrasensitive, Stretchable Strain Sensors Based on Fragmented Carbon Nanotube Papers. *ACS Appl. Mater. Interfaces.* **2017**, 9, 4835-4842.

(24) Liu, Q.; Chen, J.; Li, Y.; Shi, G. High-Performance Strain Sensors with Fish-Scale-Like Graphene-Sensing Layers for Full-Range Detection of Human Motions. *ACS Nano* **2016**, 10, 7901–7906.

(25) Lin, L.; Wang, L.; Li, B.; Luo, J.; Huang, X.; Gao, Q.; Xue, H.; Gao, J. Dual Conductive Network Enabled Superhydrophobic and High Performance Strain Sensors with Outstanding Electro-Thermal Performance and Extremely High Gauge Factors. *Chem. Eng. J.* **2020,** 385, 123391.

(26) Li, Q.; Wang, K.; Gao, Y.; Tan, J. P.; Wu, R. Y.; Xuan, F. Z. Highly Sensitive Wearable Strain Sensor Based on Ultra-Violet/Ozone Cracked Carbon Nanotube/Elastomer. *Appl. Phys. Lett.* **2018**, 112, 263501.

(27) Chen, S.; Wu, R.; Li, P.; Li, Q.; Gao, Y.; Qian, B.; Xuan, F. Acid-Interface Engineering of Carbon Nanotube/Elastomers with Enhanced Sensitivity for Stretchable Strain Sensors. *ACS Appl. Mater. Interfaces.* **2018**, 10, 37760-37766.

(28) Chen, Y.; Wang, L.; Wu, Z.; Luo, J.; Li, B.; Huang, X.; Xue, H.; Gao, J. Super-Hydrophobic, Durable and Cost-Effective Carbon Black/Rubber Composites for High Performance Strain Sensors. *Compos. Pt. B-Eng.* **2019**, 176, 107358.

(29) Muth, J. T.; Vogt, D. M.; Truby, R. L.; Menguc, Y.; Kolesky, D. B.; Wood, R. J.; Lewis, J. A. Embedded 3D Printing of Strain Sensors within Highly Stretchable Elastomers. *Adv. Mater.* **2014**, 26, 6307-12.

(30) Sun, S.; Liu, Y.; Chang, X.; Jiang, Y.; Wang, D.; Tang, C.; He, S.; Wang, M.; Guo, L.; Gao, Y. J. A Wearable, Waterproof, and Highly Sensitive Strain Sensor Based on Three-Dimensional Graphene/Carbon Black/Ni Sponge for Wirelessly Monitoring Human Motions. *J. Mater. Chem. C.* **2020**, 8, 2074-2085.

(31) Sheng, P.; Abeles, B.; Arie, Y. Hopping Conductivity in Granular Metals. *Phys. Rev. Lett.* **1973**, 31, 44-47.

(32) Chen, M.; Luo, W.; Xu, Z.; Zhang, X.; Xie, B.; Wang, G.; Han, M. An Ultrahigh Resolution Pressure Sensor Based on Percolative Metal Nanoparticle Arrays. *Nat. Commun.* **2019**, 10, 1-9.

(33) Wang, L.; Chen, Y.; Lin, L.; Wang, H.; Huang, X.; Xue, H.; Gao, J. Highly stretchable, anti-corrosive and wearable strain sensors based on the PDMS/CNTs decorated elastomer nanofiber composite. *Chem. Eng. J.* **2019**, 362, 89-98.

(34) Li, B.; Luo, J.; Huang, X.; Lin, L.; Wang, L.; Hu, M.; Tang, L.; Xue, H.; Gao, J.; Mai, Y.-W. A highly stretchable, super-hydrophobic strain sensor based on polydopamine and graphene reinforced nanofiber composite for human motion monitoring. *Compos. Pt. B-Eng.* **2020**, 181, 107580.

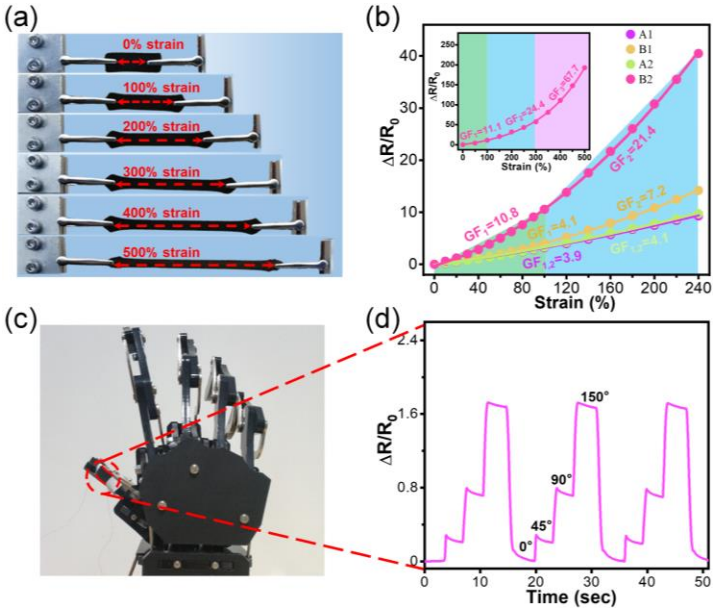
(a)
0% strain
100% strain
200% strain
300% strain
400% strain
500% strain
(b)
A1
B1
A2
B2
ΔR/R0
Strain (%)
GF1=10.8
GF1=21.4
GF2=1.2
GF2=4.1
GF1=3.9
GF2=4.1
GF=11.1
GF=24.4
GF=67.1
(c)
(d)
ΔR/R0
Time (sec)
0°
45°
90°
150°